

Review

The Importance of Apparent pKa in the Development of Nanoparticles Encapsulating siRNA and mRNA

Pratikkumar Patel,¹ Nurudeen Mohammed Ibrahim,¹ and Kun Cheng^{1,*}

Polymer and lipid nanoparticles have been extensively used as carriers to address the biological barriers encountered in siRNA and mRNA delivery. We summarize the crucial role of nanoparticle charge and ionizability in complexing RNAs, binding to biological components, escaping from the endosome, and releasing RNAs into the cytoplasm. We highlight the significant impact of the apparent pKa of nanoparticles on their efficacy and toxicity, and the importance of optimizing pKa in the development of lead formulations for RNAs. We also discuss the feasibility of fine-tuning the pKa in nanoparticles and the applications of this approach in the optimization of delivery systems for RNAs.

Delivery Systems for RNA-Based Therapeutics

RNAs are rapidly expanding as a new class of therapeutics for novel druggable molecular targets including proteins, RNAs, and genomes [1]. In particular, siRNAs and mRNAs have attracted the most attention as RNA therapeutics for a wide variety of diseases. siRNAs are 21–25 bp double-stranded non-coding RNAs that induce specific cleavage of their target mRNAs in the cytoplasm [2]. Several siRNA therapeutics have entered clinical trials, and three (Onpattro, Givlaari, and Oxlumo) have been FDA-approved for the treatment of genetic diseases. Whereas siRNAs are relatively small, with a molecular weight of ~14 kDa, mRNAs are long single-stranded RNAs with a wide range of molecular weights, from 300 kDa to 5000 kDa [3]. siRNAs are chemically synthesized, whereas mRNAs are synthesized by *in vitro* transcription (IVT; see Glossary). After entering the cells, mRNAs express encoded proteins to produce a rapid but transient therapeutic effect [4]. mRNA-based therapies have been investigated in clinical trials as cancer therapies, treatments for genetic diseases, protein replacement therapies, and vaccines [5]. Very recently, two mRNA-based vaccines against coronavirus disease 2019 (COVID-19) have been approved by the FDA, and this breakthrough has spurred global interest in mRNA-based therapies. Antigens produced by mRNA vaccines exhibit a more natural representation to the immune system, which leads to better T cell responses compared to conventional viral vector-based vaccines [6].

RNA-based therapeutics are very promising because they do not require nuclear transportation and have a low risk for mutagenesis compared to DNA-based medicines [7]. The intact form of siRNAs and mRNAs should be delivered into target cells to exert their therapeutic effect [8]. However, the negative charge and the large size of RNAs prevent their cellular entry [9]. In addition, naked RNAs are highly susceptible to nuclease degradation as well as to renal clearance in the human body. Exogenous RNAs can also be detected by the innate immune system and trigger immune responses [10]. A robust and safe delivery system is therefore essential to translate RNA-based therapeutics from bench to bedside.

Highlights

siRNA and mRNA (RNAs) therapeutics have a high potential in revolutionizing the field of medicine.

Clinical translation of RNAs is limited by their poor *in vivo* stability. The major challenge is the safe and efficient delivery of RNAs into the cytoplasm to produce the therapeutic effect.

Physicochemical optimization of RNA delivery systems is essential to enhance the effectiveness and eliminate the toxicity associated with the carriers.

The charged state of the amine groups in nanoparticles depends on the pH of the medium, and the changes can be predicted from their apparent pKa. The measurement of pKa helps in understanding the advantages and problems of the nanoparticles in various biological processes that have distinct pH values.

Optimization of nanoparticles based on their apparent pKa dramatically increases the delivery efficiency of siRNA and mRNA.

¹Division of Pharmacology and Pharmaceutical Sciences, School of Pharmacy, University of Missouri – Kansas City, 2464 Charlotte Street, Kansas City, MO 64108, USA

*Correspondence:
chengkun@umkc.edu (K. Cheng).

Chemical modification and encapsulation in nanoparticles are commonly used to overcome the biological barriers of RNA therapeutics *in vivo*. Chemical modification of RNAs has been extensively reviewed elsewhere [11], and this review focuses on nanoparticles which have been widely used for the delivery of plasmid DNA, oligonucleotides, and RNAs. Positively charged nanomaterials form nanoparticles with anionic RNAs to protect RNAs from nucleases and to help in binding to and penetrating the negatively charged cell membrane [12]. However, endosomal escape and dissociation of RNAs from the nanoparticles in the cytoplasm are the two major challenges that need to be overcome to achieve the maximum **therapeutic index** [13,14].

Among different types of nanomaterials, lipids and polymers stand out as the most commonly used nanomaterials for delivering RNAs because of their safety, flexibility, and efficiency [12,15]. A great variety of lipids and polymers with different compositions and physicochemical properties have been developed to construct nanoparticles encapsulating RNAs [16,17]. Particle size, shape, surface charge, surface area, ionization constant, and aggregation of nanoparticles are the key characteristics that determine the efficacy and safety of the nanoparticles [18–20]. Optimization of these characteristics is therefore essential to develop a successful nanoparticle formulation for RNAs.

Nanoparticles bearing ionizable amine headgroups represent a promising platform for RNA delivery [21,22]. The **acid dissociation constant** (pKa) is one of the most important physicochemical properties of the ionizable headgroups of the nanoparticles. The pKa determines the ionization behavior and surface charge of the nanoparticles, which substantially influences their stability, potency, and toxicity [8]. Their biological performance depends on the interactions of cationic nanoparticles with negatively charged blood proteins and cell membranes. These interactions are strongly influenced by the charge state of the nanoparticles' amine headgroups [23]. In addition, surface charge affects the cellular uptake, endosomal release, and biodistribution of nanoparticles [24,25]. Although a wide variety of lipids and polymers have been developed for RNA delivery, very few are optimized using pKa as a tool to achieve the highest therapeutic index. In this review we summarize the importance, applications, tuning, and measurement techniques of the pKa of nanoparticles encapsulating RNAs. We hope that the information presented in this review will facilitate the design and optimization of nanoparticles for RNA-based therapeutics.

Apparent pKa – Basics and Measurement Techniques

Apparent pKa is an experimentally determined value of molecules or nanoparticles. This value is the pH at which the numbers of ionized (protonated) and deionized groups are equal in the system. The surface charge and ionic interaction of assembled nanomaterials in nanoparticles can be estimated according to the apparent pKa. The apparent pKa of a nanoparticle is the result of the average ratio of all the ionized to deionized groups in the nanoparticle. Thus, apparent pKa is not the intrinsic pKa value of any individual molecule [26,27]. The ionizable amine groups of nanoparticles transform from deprotonated to protonated states as the pH decreases. This transition occurs very rapidly near the apparent pKa value (Box 1). A graph of apparent pKa provides information about the charge state of nanoparticles at various pH values.

The value of apparent pKa can be strongly influenced by various noncovalent interactions and environmental parameters, such as ionic strength, dielectric constant, hydrophobic interactions, π - π stacking interactions, and the presence of neighboring charges [23,28]. In addition, the apparent pKa value of the ionizable ligand-modified nanoparticles changes with nanoparticle size and shape [29]. These structural and environmental factors affect the actual ionization of nanoparticles. Thus, the apparent pKa of nanoparticles is generally lower than the calculated pKa of the individual molecules or monomers in the nanoparticles.

Glossary

Acid dissociation constant (pKa):

the pH at which molecules are half dissociated. pKa is of utmost importance for understanding drug absorption and biodistribution in the systemic circulation. pKa measurements enable the proportion of the molecules in the ionized (charged) or deionized state to be determined.

In vitro transcription:

cell-free enzymatic transcription of mRNAs from a linearized DNA or a PCR template using RNA polymerase. The template contains a bacteriophage promoter, a 5'-untranslated region (UTR), an open reading frame, a 3'-UTR, and optionally a poly(A) tail.

Median effective dose (ED₅₀):

the dose of siRNA for 50% gene silencing with an optimized lipid nanoparticle (LNP) formulation.

Sharp pH transition:

rapid protonation of all ionizable groups occurs within a narrow pH range.

Therapeutic index:

the ratio of median lethal dose to median effective dose. The relative safety of a drug is quantitatively measured by the therapeutic index.

Box 1. Measurement of Apparent pKa

The apparent pKa of nanoparticles can be measured by different techniques. Acid-base titration and 2-(*p*-toluidino)-6-naphthalene sulfonic acid (TNS) fluorescence methods are widely used in the determination of apparent pKa of blank nanoparticles. In the acid-base titration (also known as potentiometric titration) method, the blank nanoparticles are first suspended in 0.1M HCl solution, and titration is carried out by adding 0.1 M NaOH or 0.5 M KOH solution. The pKa value is determined as the pH in the midpoint of the two equivalence points of the titration curve [85]. Figure 1A shows a schematic illustration of the titration curve for ionizable amine-bearing nanoparticles. Automatic instruments, such as SiriusT3, are available to carry out the acid-base titration experiment at a small scale [23,86].

The TNS fluorescence method is very sensitive and has been extensively used to measure the pKa of LNPs [32]. TNS is non-fluorescent in aqueous solutions but exhibits strong fluorescence after it binds to cationic lipids or polymers and moves to hydrophobic environment [23,87]. As the pH decreases, the interaction between TNS and the cationic surface increases, leading to a steady increment in fluorescence. The fluorescence reaches a maximum when all the ionizable groups are charged at a specific pH [49]. To carry out the TNS fluorescence assay, a series of buffer solutions are prepared in the pH range 3–10 using 150 mM NaCl, 10 mM borate, 10 mM phosphate, and 10 mM citrate. Blank nanoparticles are prepared and diluted in each buffer solution. TNS is dissolved in dimethyl sulfoxide (DMSO) at 300 μ M, and 2 μ l of the TNS solution is mixed with 100 μ l of blank nanoparticles. The fluorescence is then measured at the excitation and emission wavelengths of 325 nm and 435 nm, respectively [8]. Figure 1B shows a schematic of the fluorescence as a function of pH.

The fluorescence of TNS relies on the binding of TNS to positively charged lipids. TNS binding to the lipids is limited by the accessibility of the positively charged lipid headgroups, which are relatively smaller compared to TNS. TNS fluorescence increases steadily with the concentration of lipids before it reaches a plateau [23]. It is noted that it is challenging to observe lower pKa values for lipids bearing multiple amines because of steric hindrance of TNS [23]. However, if TNS is not completely utilized in the first inflection we can see a small inflection in fluorescence at lower pKa values for lipids with multiple amines [48]. Similarly, the double sigmoidal ionization curve of lipids with two ionizable amines was normalized to the net charges of lipid against pH range using the single cationic DOTAP (dioleoyltrimethylammoniumpropane) and uncharged DOPC (dioleoylphosphatidylcholine) nanoparticles. The net charge values are greater than 1.0, suggesting that both the ionizable amines of the lipid respond to TNS [88].

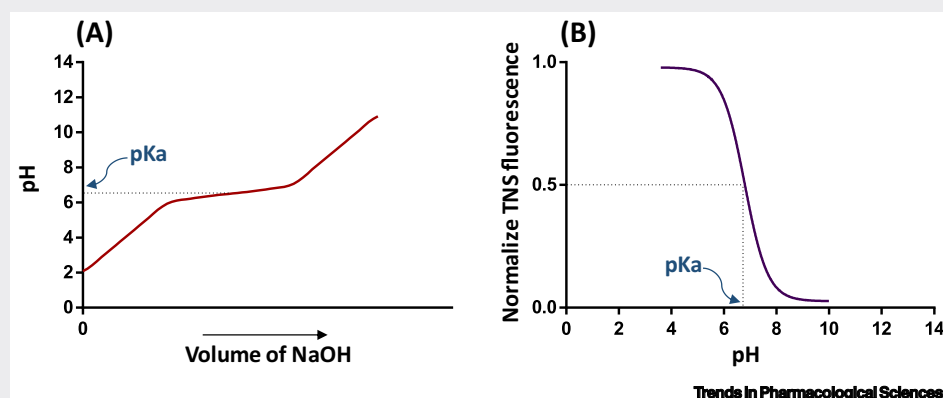


Figure 1. Schematic Diagram of Methods for pKa Measurement. (A) Potentiometric titration of nanoparticles (in an acidic solution) with base to incrementally increase the pH. The deionization of the nanoparticles inflects the titration curve by producing buffer action. The middle of the two equivalence points represents the pKa of the nanoparticles. (B) TNS fluorescence measurement of nanoparticles at various pH values shows the fluorescence corresponding to the ratio of ionized to deionized amines. TNS interacts with positively charged amines and produces a fluorescence signal. The pH value at the half-maximum value of fluorescence represents the pKa of the nanoparticles.

Apparent pKa in Nanoparticle-Based RNA Delivery

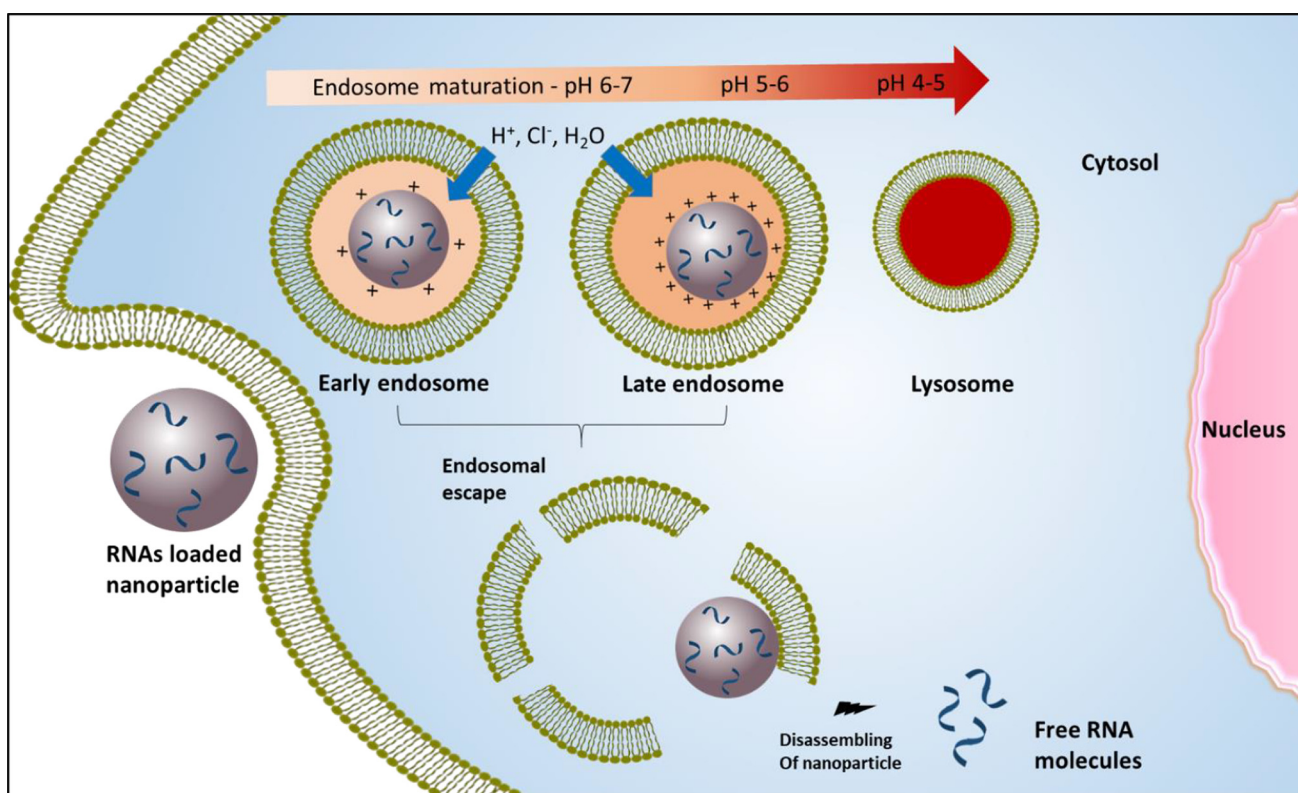
The apparent pKa value reflects the charge interaction behavior of nanoparticles, which significantly affects their biological activity because the positively charged molecules of the nanoparticles can interact with negatively charged proteins and cells in the body [30]. Negatively charged RNAs condense with ionizable cationic nanomaterials to form nanoparticles by electrostatic interactions, thus protecting RNAs from nuclease degradation [31]. Nanoparticles with an optimum pKa carry negligible

charge at physiological pH, thereby preventing nonspecific binding and toxicity in the body [32]. In addition, the optimum pKa of nanoparticles plays important roles in endosomal escape and in RNA release into the cytosol to exert therapeutic effect (Figure 1) [33–36].

Toxicity, inefficient endosomal escape, and inadequate dissociation of RNAs from nanoparticles in the cytoplasm are the major challenges that are correlated to the charge state of the nanoparticles, and these challenges can be overcome by tuning the apparent pKa. Therefore, the apparent pKa is the most important parameter to improve the efficacy of nanoparticles encapsulating RNAs [23,32,37].

Apparent pKa of Lipid Nanoparticles in siRNA Delivery

Lipid nanoparticles (LNPs) are the most clinically advanced drug-delivery systems for RNA delivery [38]. LNPs are composed of a mixture of ionizable or cationic lipid, phospholipid, polyethylene glycol (PEG)-lipid, and cholesterol [39]. Although ionizable lipid is the major and most important component of LNPs, other components also affect the stability and function of LNPs [40]. Patisiran (ONPATTRO™) is the first-ever FDA-approved siRNA therapy [41], and the transthyretin (TTR)-



Trends in Pharmacological Sciences

Figure 1. Delivery of RNAs into the Cytoplasm through Endosomal Escape with Ionizable Nanoparticles. Once nanoparticles are taken up by the cells, the charges on the nanoparticle increase as the pH decreases below the pKa during endosomal maturation (pH 7–5.5). Nanoparticles with a pKa in this range are protonated due to the acceptance of protons by amine groups. The accumulation of protons with counterions enhances the transportation of liquids from the cytosol to the endosome to counteract the osmotic pressure. The rapid ionization of nanoparticles near the pKa creates a buffering capacity which accounts for the proton sponge effect. Osmotic swelling, due to the buffering capacity of nanoparticles and/or membrane destabilization (owing to interaction of the negatively charged endosome bilayer with positively charged lipids or polymers of nanoparticle, leads to bursting of endosomes. The charges on nanoparticles decrease in the cytosol and weaken the binding interaction with RNAs. Finally, the nanoparticles dissociate to release the RNAs and produce the desired activity.

targeted siRNA is encapsulated in LNPs composed of the DLin-MC3-DMA [heptatriacontetraene-19-yl 4-(dimethylamino)butanoate, also known as MC3] lipid [42].

The MC3 lipid was developed with rational design approaches by systematically varying the structure of lipid 1,2-dilinolexyloxy-3-dimethylaminopropane (DLinDMA). The two double bonds in each tail are responsible for the high gene-silencing activity of DLinDMA. The degree of saturation of the lipids affects the phase-transition temperature of LNPs. The increase in the number of double bonds from zero to two in the tail decreases the phase-transition temperature and enhances the fusogenicity of the lipids [43]. Later, the DLin-K-DMA lipid was developed by introducing a ketal ring into the linker of DLinDMA, which increased the silencing activity by 2.5-fold. The activity was further enhanced by incorporating an additional methylene group between the ketal ring and ionizable amine, resulting in the DLin-KC2-DMA (KC2) lipid. KC2 LNPs with a pKa of 6.7 showed a potent *in vivo* activity with a **median effective dose** (ED₅₀) of 0.1 mg/kg [35]. Finally, the MC3 lipid was discovered by screening 53 analogs of a highly potent KC2 lipid. These analogs were synthesized in the pKa range 4.17–8.12 by varying the headgroup of the lipid KC2. A strong correlation was found between the apparent pKa and *in vivo* activity [32]. The gene-silencing activity of all the LNPs was evaluated in female C57BL/6 mice after intravenous (IV) administration. A plot of pKa versus ED₅₀ shows a strong correlation between pKa and *in vivo* FVII gene-silencing activity, and MC3 LNPs (pKa 6.44) exhibit an ED₅₀ of 0.03 mg/kg. The formulation was further optimized by varying the ratio of co-lipids, resulting in an ED₅₀ of 0.005 mg/kg. According to the results, a pKa of 6.2–6.5 is the optimum range for maximum activity [32]. The MC3 lipid was further modified by adding an ester linkage at different sites on the aliphatic chain to improve biodegradability and safety. The modified lipids from MC3 with pKa values in the range 6.2–6.4 demonstrated promising activity for hepatic gene silencing. The highly active biodegradable lipid L319 has an ED₅₀ value of less than 0.01 mg/kg [44].

Another approach to developing highly effective lipids is to screen a large combinatorial library of lipid-like molecules [45,46]. For example, a library containing 1400 lipids was screened using *in vitro* gene-silencing study, and 96 lipids that showed >50% silencing activity were further evaluated for *in vivo* activity. Fifteen lipids that showed effective gene-silencing activity in mice had pKa values >5.5. The lead compound 304O₁₃ was identified based on its good liver biodistribution and gene-silencing activity. 304O₁₃ has a pKa value of 6.8. Other lead compounds, including 306O₁₂ and 113O₁₃, have pKa values of 6.8 and 6, respectively. However, their biodistribution profiles were relatively poor compared to 304O₁₃ [47]. This combinatorial approach was also used to screen another lipid library for delivery of siRNAs into leukocytes. Lipids with a piperazine head group accumulated more in the spleen compared to the liver. 'Lipid 10' has a pKa in the range 6.2–6.5 and showed significant gene-silencing activity in animal studies [48].

To understand the effect of particle size, lipase sensitivity, and pKa on the biodistribution, cell specificity, and gene silencing activity of LNPs in the liver, six novel lipids were developed by modifying the headgroup of a previously synthesized pH-sensitive lipid, YSK05 [49]. The plot of ED₅₀ against pKa showed a bell-shaped curve for FVII gene silencing in hepatocytes, and the lipid with the highest activity has a pKa of 6.45. By contrast, silencing of CD31 in liver sinusoidal endothelial cells exhibited a sigmoidal curve, showing that gene-silencing activity increases with pKa up to 7 [49]. This result suggests that tuning the pKa of LNPs can be used to achieve cell-specific activity.

In another study, multiple parameters (particle size, siRNA entrapment, stability, pKa, hemolysis, and cellular uptake) of LNPs were studied to understand how they affect *in vitro* and *in vivo* silencing activity [8]. The results indicate that increased cellular uptake did not always correlate with increased silencing activity. LNPs should not dissociate before cellular entry, and they must escape the endosome to release siRNAs in an intact form to produce the silencing effect.

Gene-silencing activity is more highly correlated with pKa than with particle size and siRNA entrapment. LNPs with a pKa between 6 and 7 showed promising gene silencing, whereas LNPs with pKa between 3 and 6 exhibited poor stability and cellular uptake, resulting in poor silencing activity [8]. Another study showed the impact of structural changes on physicochemical parameters and *in vivo* activity. Nanoparticles with a pKa of 6–6.6 and a calculated lipophilicity of 10–14 showed good *in vivo* activity [50].

Apparent pKa of Lipid Nanoparticles for mRNA Delivery

The recent success of two mRNA-based vaccines for COVID-19 has drawn increasing interest in mRNA therapy. Compared to conventional vaccines, it is much faster to develop mRNA-based vaccines, allowing us to promptly respond to virus outbreaks [4,51]. Lipids SM-102 (lipid H) and ALC-0315 are used in the formulation of Moderna's COVID-19 vaccine (mRNA-1273) and Pfizer's vaccine (BNT162b2 RNA), respectively^{i,ii}.

Various routes of administration were evaluated for mRNA vaccines, and intramuscular (IM), intradermal, and subcutaneous administrations produced robust protein expression at the site of injection [52,53]. To develop a highly efficient delivery system for mRNA vaccines, Moderna synthesized 30 lipids and compared their efficacy to the MC3 lipid [6]. Among the 14 lipids that yielded a higher α -H10 IgG titer than MC3, only four lipids showed higher luciferase expression relative to MC3, but another four lipids exhibited lower luciferase expression than MC3. This interesting result suggests that protein expression upon IM administration cannot predict immunogenicity. By contrast, the pKa of LNPs is a strong determinant of the immunogenicity, and the optimum pKa range is 6.6–6.9 for IM delivery. 'Lipid H' (pKa 6.68) was finally selected as the best lipid to deliver mRNA vaccines because of its good biodegradability, tolerability, protein expression, and immunogenicity [6]. Later, the lipid H (SM-102) was used for the COVID-19 vaccine 'mRNA-1273'.

LNPs that were originally designed for siRNA delivery can be modified to deliver mRNAs. For example, the C12-200 LNP designed for siRNAs was optimized by simultaneously varying the lipid ratios and structures. The optimized C12-200 LNP increased the potency of erythropoietin mRNA by sevenfold relative to the original LNP [54]. Both LNPs exhibit similar morphological characteristics except for the apparent pKa, which was changed from 7.25 to 6.96 for the optimized LNP. Interestingly, both LNPs showed similar potency in siRNA delivery, highlighting the differences in optimized formulation parameters for siRNA and mRNA [54]. Later, the same group synthesized a series of alkenyl amino alcohol (AAA) ionizable lipids for mRNA delivery by introducing different unsaturated fatty chains into the cKK-E12 lipid. The optimized lipid OF-02 yielded a twofold increase in protein expression *in vivo* compared to cKK-E12 [55].

mRNA LNP was also used to express a chimeric antigen receptor (CAR) on human T cells to overcome the side effects associated with virus-based CAR T cell therapy. Among 24 lipids, the best lipid C14-4 delivered the CD19 mRNA and produced similar amounts of CAR expression with less cytotoxicity compared to the electroporation method. In addition, the LNP from pure C14-4 has a pKa of 6.5, and the mRNA-LNP-based CAR T cell therapy elicited potent antitumor activity against Nalm-6 cells [56].

Another lipid library was constructed by reacting the alkyl-amine 306 with an alkyl-acrylate tail with different lengths [57]. The lipids with 10-carbon tails were highly effective and expressed encoded proteins in mice after IV injection. Moreover, lipid '306₁₀' with a branched tail showed a ten-fold improvement in efficiency compared to lipid '306₁₀' which contains a straight tail. The improved efficacy of lipid '306₁₀' is due to its high surface ionization in the late endosome [57].

Table 1. Highly Effective Lipids and Polymers for RNA Delivery

Number	Name	pKa	Structure	Delivery material (route)	ED ₅₀ ^a (mg/kg)	Refs
1	DlinDMA	6.8		siRNA (IV)	1	[35]
2	Dlin-KC2-DMA	6.68		siRNA (IV)	0.02	[35]
3	Dlin-MC3-DMA	6.44		siRNA mRNA (IV)	0.005	[32]
4	L319	6.38		siRNA (IV)	<0.01	[44]
5	YSK13-C3	6.45		siRNA (IV)	0.015	[89]
6	304O ₁₃	6.8		siRNA (IV)	0.01	[47]
7	503O ₁₃	5.5–7 ^b		siRNA (IV)	0.01	[47]
8	CKK-E12	N.A. ^c		siRNA (IV)	0.002	[45]
9	C12-200	6.96		siRNA mRNA (IV)	N.A.	[56]

(continued on next page)

Table 1. (continued)

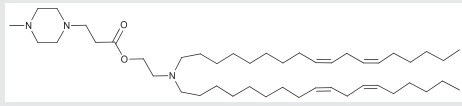
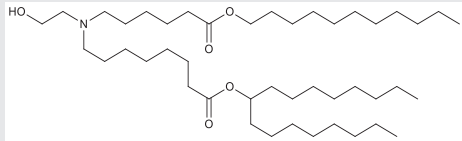
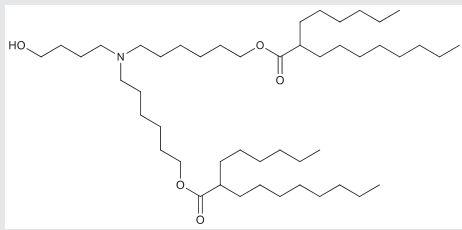
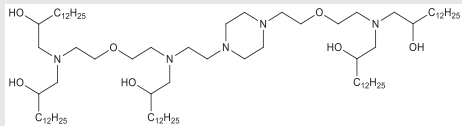
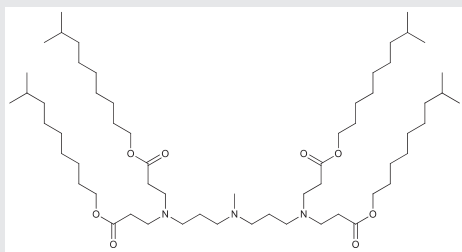
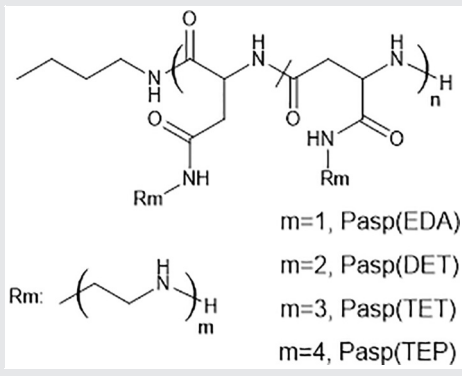
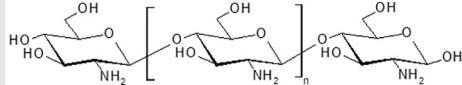
Number	Name	pKa	Structure	Delivery material (route)	ED ₅₀ ^a (mg/kg)	Refs
10	Lipid 10	6.2–6.5 ^b		siRNA (IV)	N.A.	[48]
11	Lipid H (SM-102)	6.68		mRNA (IM)	N.A.	[6]
12	ALC-0315	6.09		mRNA (IM)	N.A.	[90] ⁱⁱ
13	C14-4	6.51		mRNA	N.A.	[56]
14	306 ₁₀	6.4		mRNA (IV)	N.A.	[57]
15	Pasp(EDA) Pasp(DET) Pasp(TET) Pasp(TEP)	pKa1: 9 pKa1: 8.9 pKa2: 6.2 pKa1: 9.1 pKa2: 7.8 pKa3: 4.3 pKa1: 9.0 pKa2: 8.2 pKa3: 6.3		siRNA mRNA	N.A.	[68] [69,70]
16	Chitosan	~6.5		siRNA mRNA (IV)	N.A.	[73–75]

Table 1. (continued)

Number	Name	pKa	Structure	Delivery material (route)	ED ₅₀ ^a (mg/kg)	Refs
17	EAASc EAASd	5.8 6.0	<p>EAASc: $x=40, y=36, z=37$, Rm: , Rm': </p> <p>EAASd: $x=40, y=35, z=35$, Rm: , Rm': </p>	siRNA (IV)	N.A.	[77]
18	PDPA ₈₀	6.24	<p>PDPA₈₀: $x=80$</p>	siRNA (IV)	N.A.	[79]

^aThe ED₅₀ value is the dose of siRNA for 50% FVII gene silencing in mice using an optimized LNP formulation.

^bThe exact pKa values for lipid 503O₁₃ and lipid 10 have not been reported.

^cN.A., not available.

Apparent pKa of Polymeric Nanoparticles for RNA Delivery

Numerous polymer-based nanomedicines have been approved by the FDA [58]. A wide range of cationic, ionizable, biodegradable, and charge-altering polymers have been used in the preparation of nanoparticles for effective delivery of RNAs [59–61]. The physicochemical properties (size, surface charges, stability, entrapment, and toxicity) of polymers can be optimized by modifying the ionizable groups or by varying the size of polymers. Controlling these physicochemical characteristics allows the creation of an efficient polymeric delivery system for RNA therapeutics [62].

Polyethyleneimine (PEI) has been extensively used in DNA and RNA delivery because of its endosomal escape capability [63]. The protonation of amines produces a proton sponge effect in early endosomes [63]. However, PEI carries a positive charge in physiological conditions, and its interaction with biomolecules induces significant toxicity [64]. As a result, PEIs have been modified with various biomaterials to reduce their toxicity [65,66]. For example, a specified number (1–4) of aminoethylene units, such as ethylenediamine (EDA), diethylenetriamine (DET), triethylenetetramine (TET), and tetraethylenepentamine (TEP), were introduced into polyaspartamides (Pasp) to form cationic copolymers with reduced toxicity [67]. Pasp(DET) and Pasp(TEP) have amine regions with pKa values of 6.2 and 6.3, respectively. Both polymers exhibit increased protonation in the endosome, leading to efficient endosomal escape. These polymers were subsequently used for the delivery of siRNA [68]. Moreover, these polymers were modified with PEG and cholesterol (Chol) to form PEG-Pasp(DET) and PEG-Pasp(TEP)-Chol for mRNA delivery to the central nervous system (CNS) and for the treatment of pancreatic cancer, respectively [69,70].

Chitosan is another well-characterized and extensively used polymer in RNA delivery [71]. The pKa of chitosan is in the range 6.2–7.0 and can be influenced by the molecular weight and degree of deacetylation [72]. Thus, chitosan-based nanoparticles are safe and effective in delivering siRNAs and mRNAs [73–75]. Moreover, chitosan can be easily modified to meet the specific

requirements of RNA delivery because each subunit of chitosan has two hydroxyl groups and one amine group [76].

The relationship between pKa and siRNA delivery efficiency was studied in tri-block copolymers which have been widely used for RNA delivery. A series of triblock copolymers with pKa values ranging from 5.2 to 7.0 were synthesized by adjusting the number and type of hydrophobic amine monomers. The copolymers with a pKa of 5.8–6.2 showed a better gene-silencing effect. The lead copolymer, EAASc, exhibited high silencing effect in MDA-MB-231 (92.45%), HepG2 (89.94%), 293A (83.06%), and HeLa cells (80.27%). The polymer also showed silencing activity in tumors after peritumoral injection [77].

pH-responsive polymers are another promising type of carrier for RNA delivery. The pH response is a result of the reversible deprotonation and protonation of ionizable groups. pKa is a crucial parameter to reflect the ionization status of nanoparticles at various pH values. Nanoparticles with optimum pKa values exhibit maximum efficacy by responding to endosomal pH [78]. For example, a series of poly(2-(diisopropylamino)ethylmethacrylate) (PDPA)-based ultra-pH-sensitive polymers were evaluated for siRNA delivery. Among them, PDPA₈₀ has a pKa of 6.24 and showed excellent gene silencing through the proton sponge effect. siRNA nanoparticles made of the polymer exhibited excellent anticancer activity *in vivo* [79]. The preservation of pH sensitivity at an optimum level in nanostructures is highly significant for generating maximum endosomal escape and RNA efficacy.

Tuning the pKa of Nanoparticles

The apparent pKa of polymeric nanoparticles can be tuned by chemically modifying monomers, changing the molar ratio of different monomers in a copolymer, or changing the molecular weight of a polymer. For example, an ultra-pH-sensitive nanoprobe library was developed using two randomly distributed monomer R1 and R2 in PEO-b-P(R1-r-R2). The polymers polyethyleneoxide-b-poly(2-(dibutylamino)ethylmethacrylate) (PEO-b-PDBA) and PEO-PDPA (propyl) have pKa values of 5.3 and 6.2, respectively. The molar ratio of the monomers DBA and DPA was precisely controlled in the polymerization process to synthesize a series of PEO-b-P(DPA-r-DBA) polymers with a pKa in the range of 5.3–6.2. Similarly, another series of polymers were synthesized by controlling the polymerization of monomer DEA (ethyl) with DPA and D5A (pentyl) with DBA. The nanoprobe library covered the pH range of 4–7.4. The **sharp pH transition** of nanoprobes is strongly correlated with their apparent pKa [80].

The apparent pKa of LNPs is dependent not only on the pKa of individual lipid but also on the molar ratio of all the lipids. Each lipid has a distinct pKa which can be changed by modifying its headgroup and the hydrophobic tail [44]. Therefore, one strategy to adjust the apparent pKa of LNPs is to chemically modify the lipid. Another strategy is to use a mixture of two or more lipids with different pKa values and adjust their ratio to achieve the desirable apparent pKa. For example, LNPs with pKa values between 5.64 and 6.93 were developed by mixing various ratios of two of the three structurally similar lipids, 15 (pKa 5.64), 16 (pKa 6.44), and 17 (pKa 6.93) [32]. Similarly, various ratios of lipids YSK05 (pKa 6.50) and YSK12-C4 (pKa 8.00) were mixed to form LNPs with apparent pKa values ranging between 6.50 to 8.00 [81].

Concluding Remarks and Future Perspectives

The key requirement for successful RNA therapy is to overcome the extracellular and intracellular barriers that may degrade RNAs before they reach the site of action. Although nanoparticles have been extensively used to protect RNAs from degradation, endosomal entrapment of the nanoparticles is a major bottleneck that limits the therapeutic effect. The mechanism of endosomal

Outstanding Questions

What is the best strategy to develop or optimize siRNA- and mRNA-based formulations?

What are the best ways to improve the therapeutic index of nanoparticle-based RNA therapeutics?

What is the importance of measuring the apparent pKa of nanoparticles?

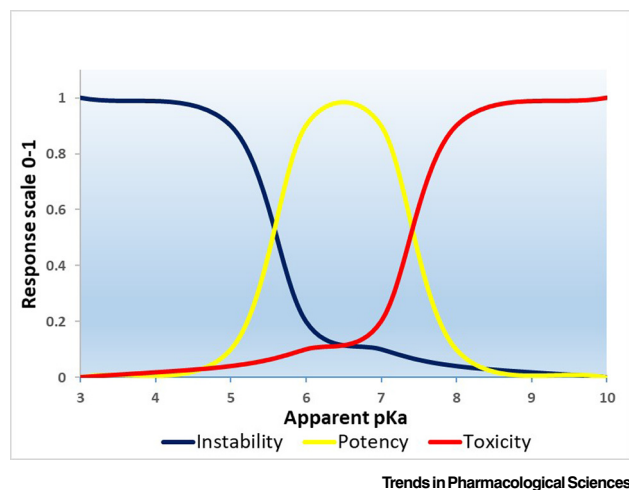


Figure 2. The Effects of pKa on the Instability, Potency, and Toxicity of Nanoparticles. The graph represents the normal behavior of ionizable cationic nanoparticles with different pKa values in biological systems. An apparent pKa of 6–7 is the optimum range for the development of highly efficient nanoparticles for RNA delivery. Nanoparticles with lower pKa values have insufficient ionic charges and polarity at neutral pH, thereby leading to aggregation of the nanoparticles because hydrophobic interactions between the particles are stronger. They are thus less stable in biological systems. However, nanoparticles with a higher pKa carry positive charges at physiological pH, which is the main reason for their

toxicity. Most importantly, nanoparticles with lower and higher pKa values outside the range of 6–7 do not ionize effectively during endosome maturation. As a result, they cannot efficiently release their cargo into the cytoplasm.

escape is not completely understood, and it varies from one type of cell to another [82,83]. Significant efforts have been undertaken to understand the endosomal escape mechanisms of nanoparticles and to overcome endosomal entrapment with different approaches.

It is generally believed that the structural and physicochemical properties of nanoparticles play important roles in delivering RNAs [8,21,35,47,67]. However, the structural requirements for effective RNA delivery are not conclusive, and the structural features of most active lipids are very different (Table 1). By contrast, the apparent pKa of nanoparticles stands out as a reliable criterion to predict the efficiency of nanoparticles encapsulating RNAs. The apparent pKa of nanoparticles has a high correlation with their efficacy and toxicity. Nanoparticles with apparent pKa in the optimum range (see Outstanding Questions) exhibit efficient endosomal escape and therapeutic effect (Figure 2). Incorporation of apparent pKa as a design criterion in the development of nanoparticles will facilitate the discovery of effective and safe RNA therapies.

The most efficient lipid and polymer nanoparticles in RNA delivery have apparent pKa values between 6 and 7 (Table 1). LNPs with optimized pKa values of 6.2–6.5 were found to be effective for hepatic delivery of siRNAs [32]. LNPs with an optimal pKa in the range of 6.6–6.9 produced very efficient immune responses after IM administration of mRNAs [6]. The endocytotic processes differ from cells to cells because the proliferation status of cells varies with their physiological roles [84]. The apparent pKa should be optimized according to the target tissue and disease condition. Overall, the optimum pKa value depends on several factors, including the structure of the carrier, the target tissue, and the route of delivery. As a result, it is difficult to recommend a universal pKa value of nanoparticles for RNA delivery. Nevertheless, it would be appropriate to say that an optimum pKa range of 6–7 is the ideal range for the development of nanoparticles for RNA therapeutics.

Acknowledgements

This work is supported by the National Institutes of Health (R01AA021510, R01CA231099, and R01GM121798).

Declaration of Interests

The authors declare no conflicts of interest.

Resources

ⁱ<https://clinicaltrials.gov/ct2/show/NCT04283461>

ⁱⁱwww.gov.uk/government/publications/regulatory-approval-of-pfizer-biontech-vaccine-for-covid-19/summary-public-assessment-report-for-pfizerbiontech-covid-19-vaccine

References

1. Yu, A.-M. *et al.* (2019) RNA therapy: are we using the right molecules? *Pharmacol. Ther.* 196, 91–104
2. Cheng, K. and Mahato, R.I. (2011) Biological and therapeutic applications of small RNAs. *Pharm. Res.* 28, 2961–2965
3. Tang, X. *et al.* (2010) Therapeutic prospects of mRNA-based gene therapy for glioblastoma. *Front. Oncol.* 9, 1208
4. Zhong, Z. *et al.* (2018) mRNA therapeutics deliver a hopeful message. *Nano Today* 23, 16–39
5. Wadhwa, A. *et al.* (2020) Opportunities and challenges in the delivery of mRNA-based vaccines. *Pharmaceutics* 12, 102
6. Hassett, K.J. *et al.* (2019) Optimization of lipid nanoparticles for intramuscular administration of mRNA vaccines. *Mol. Ther. Nucleic Acids* 15, 1–11
7. Gomez-Aguado, I. *et al.* (2020) Nanomedicines to deliver mRNA: state of the art and future perspectives. *Nanomaterials (Basel)* 10, 364
8. Alabi, C.A. *et al.* (2013) Multiparametric approach for the evaluation of lipid nanoparticles for siRNA delivery. *Proc. Natl. Acad. Sci. U. S. A.* 110, 12881–12886
9. Tai, W. and Gao, X. (2018) Noncovalent tagging of siRNA with steroids for transmembrane delivery. *Biomaterials* 178, 720–727
10. Kaczmarek, J.C. *et al.* (2017) Advances in the delivery of RNA therapeutics: from concept to clinical reality. *Genome Med.* 9, 60
11. Ku, S.H. *et al.* (2016) Chemical and structural modifications of RNAi therapeutics. *Adv. Drug Deliv. Rev.* 104, 16–28
12. Chahal, J.S. *et al.* (2016) Dendrimer-RNA nanoparticles generate protective immunity against lethal Ebola, H1N1 influenza, and *Toxoplasma gondii* challenges with a single dose. *Proc. Natl. Acad. Sci. U. S. A.* 113, E4133–E4142
13. Gilleron, J. *et al.* (2013) Image-based analysis of lipid nanoparticle-mediated siRNA delivery, intracellular trafficking and endosomal escape. *Nat. Biotechnol.* 31, 638–646
14. Kwon, Y.J. (2012) Before and after endosomal escape: roles of stimuli-converting siRNA/polymer interactions in determining gene silencing efficiency. *Acc. Chem. Res.* 45, 1077–1088
15. Kanasty, R. *et al.* (2013) Delivery materials for siRNA therapeutics. *Nat. Mater.* 12, 967–977
16. Kulkarni, J.A. *et al.* (2019) Lipid nanoparticle technology for clinical translation of siRNA therapeutics. *Acc. Chem. Res.* 52, 2435–2444
17. Chenthamara, D. *et al.* (2019) Therapeutic efficacy of nanoparticles and routes of administration. *Biomater. Res.* 23, 20
18. Khan, I. *et al.* (2019) Nanoparticles: properties, applications and toxicities. *Arab. J. Chem.* 12, 908–931
19. Jasinski, D.L. *et al.* (2018) The effect of size and shape of RNA nanoparticles on biodistribution. *Mol. Ther.* 26, 784–792
20. Shi, J. *et al.* (2017) Cancer nanomedicine: progress, challenges and opportunities. *Nat. Rev. Cancer* 17, 20–37
21. Akinc, A. *et al.* (2008) A combinatorial library of lipid-like materials for delivery of RNAi therapeutics. *Nat. Biotechnol.* 26, 561–569
22. Yin, H. *et al.* (2014) Non-viral vectors for gene-based therapy. *Nat. Rev. Genet.* 15, 541–555
23. Zhang, J. *et al.* (2011) Ionization behavior of amino lipids for siRNA delivery: determination of ionization constants, SAR, and the impact of lipid pKa on cationic lipid-biomembrane interactions. *Langmuir* 27, 1907–1914
24. Fromen, C.A. *et al.* (2016) Nanoparticle surface charge impacts distribution, uptake and lymph node trafficking by pulmonary antigen-presenting cells. *Nanomedicine* 12, 677–687
25. Kranz, L.M. *et al.* (2016) Systemic RNA delivery to dendritic cells exploits antiviral defence for cancer immunotherapy. *Nature* 534, 396–401
26. Tsui, F.C. *et al.* (1986) The intrinsic pKa values for phosphatidylserine and phosphatidylethanolamine in phosphatidylcholine host bilayers. *Biophys. J.* 49, 459–468
27. Cawley, J.J. (1993) The determination of 'apparent' pKa's: an experiment for liberal arts or science students. *J. Chem. Educ.* 70, 596
28. Li, Y. *et al.* (2016) Non-covalent interactions in controlling pH-responsive behaviors of self-assembled nanosystems. *Polym. Chem.* 7, 5949–5956
29. Wang, D. *et al.* (2011) How and why nanoparticle's curvature regulates the apparent pKa of the coating ligands. *J. Am. Chem. Soc.* 133, 2192–2197
30. Carnal, F. *et al.* (2016) Polypeptide–nanoparticle interactions and corona formation investigated by Monte Carlo simulations. *Polymers (Basel)* 8, 203
31. Johannes, L. and Lucchino, M. (2018) Current challenges in delivery and cytosolic translocation of therapeutic RNAs. *Nucleic Acid. Ther.* 28, 178–193
32. Jayaraman, M. *et al.* (2012) Maximizing the potency of siRNA lipid nanoparticles for hepatic gene silencing in vivo. *Angew. Chem. Int. Ed. Engl.* 51, 8529–8533
33. Gujrati, M. *et al.* (2014) Multifunctional cationic lipid-based nanoparticles facilitate endosomal escape and reduction-triggered cytosolic siRNA release. *Mol. Pharm.* 11, 2734–2744
34. Sahay, G. *et al.* (2013) Efficiency of siRNA delivery by lipid nanoparticles is limited by endocytic recycling. *Nat. Biotechnol.* 31, 653–658
35. Semple, S.C. *et al.* (2010) Rational design of cationic lipids for siRNA delivery. *Nat. Biotechnol.* 28, 172–176
36. Patel, S. *et al.* (2019) Brief update on endocytosis of nanomedicines. *Adv. Drug Deliv. Rev.* 144, 90–111
37. Maugeri, M. *et al.* (2019) Linkage between endosomal escape of LNP-mRNA and loading into EVs for transport to other cells. *Nat. Commun.* 10, 4333
38. Kulkarni, J.A. *et al.* (2018) Lipid nanoparticles enabling gene therapies: from concepts to clinical utility. *Nucleic Acid Ther.* 28, 146–157
39. Kulkarni, J.A. *et al.* (2018) On the formation and morphology of lipid nanoparticles containing ionizable cationic lipids and siRNA. *ACS Nano* 12, 4787–4795
40. Ramezanzpour, M. *et al.* (2019) Ionizable amino lipid interactions with POPC: implications for lipid nanoparticle function. *Nanoscale* 11, 14141–14146
41. Hoy, S.M. (2018) Patisiran: first global approval. *Drugs* 78, 1625–1631
42. Titze-de-Almeida, S.S. *et al.* (2020) Leading RNA interference therapeutics. Part 1: silencing hereditary transthyretin amyloidosis, with a focus on patisiran. *Mol. Diagn. Ther.* 24, 49–59
43. Heyes, J. *et al.* (2005) Cationic lipid saturation influences intracellular delivery of encapsulated nucleic acids. *J. Control. Release* 107, 276–287
44. Maier, M.A. *et al.* (2013) Biodegradable lipids enabling rapidly eliminated lipid nanoparticles for systemic delivery of RNAi therapeutics. *Mol. Ther.* 21, 1570–1578
45. Dong, Y. *et al.* (2014) Lipopeptide nanoparticles for potent and selective siRNA delivery in rodents and nonhuman primates. *Proc. Natl. Acad. Sci. U. S. A.* 111, 3955–3960
46. Love, K.T. *et al.* (2010) Lipid-like materials for low-dose, in vivo gene silencing. *Proc. Natl. Acad. Sci. U. S. A.* 107, 1864–1869
47. Whitehead, K.A. *et al.* (2014) Degradable lipid nanoparticles with predictable in vivo siRNA delivery activity. *Nat. Commun.* 5, 4277
48. Ramishetti, S. *et al.* (2020) A combinatorial library of lipid nanoparticles for RNA delivery to leukocytes. *Adv. Mater.* 32, e1906128
49. Sato, Y. *et al.* (2016) Relationship between the physicochemical properties of lipid nanoparticles and the quality of siRNA delivery to liver cells. *Mol. Ther.* 24, 788–795

50. Rajappan, K. *et al.* (2020) Property-driven design and development of lipids for efficient delivery of siRNA. *J. Med. Chem.* 63, 12992–13012
51. Pardi, N. *et al.* (2018) mRNA vaccines – a new era in vaccinology. *Nat. Rev. Drug Discov.* 17, 261–279
52. Pardi, N. *et al.* (2015) Expression kinetics of nucleoside-modified mRNA delivered in lipid nanoparticles to mice by various routes. *J. Control. Release* 217, 345–351
53. Bahl, K. *et al.* (2017) Preclinical and clinical demonstration of immunogenicity by mRNA vaccines against H10N8 and H7N9 influenza viruses. *Mol. Ther.* 25, 1316–1327
54. Kauffman, K.J. *et al.* (2015) Optimization of lipid nanoparticle formulations for mRNA delivery in vivo with fractional factorial and definitive screening designs. *Nano Lett.* 15, 7300–7306
55. Fenton, O.S. *et al.* (2016) Bioinspired alkenyl amino alcohol ionizable lipid materials for highly potent in vivo mRNA delivery. *Adv. Mater.* 28, 2939–2943
56. Billingsley, M.M. *et al.* (2020) Ionizable lipid nanoparticle-mediated mRNA delivery for human CART T cell engineering. *Nano Lett.* 20, 1578–1589
57. Hajj, K.A. *et al.* (2019) Branched-tail lipid nanoparticles potently deliver mRNA in vivo due to enhanced ionization at endosomal pH. *Small* 15, e1805097
58. Ventola, C.L. (2017) Progress in nanomedicine: approved and investigational nanodrugs. *Pharm. Ther.* 42, 742–755
59. Wu, C. *et al.* (2018) Rationally designed polycationic carriers for potent polymeric siRNA-mediated gene silencing. *ACS Nano* 12, 6504–6514
60. McKinlay, C.J. *et al.* (2017) Charge-altering releasable transporters (CARTs) for the delivery and release of mRNA in living animals. *Proc. Natl. Acad. Sci. U. S. A.* 114, E448–E456
61. Ben Djemaa, S. *et al.* (2019) Versatile electrostatically assembled polymeric siRNA nanovectors: can they overcome the limits of siRNA tumor delivery? *Int. J. Pharm.* 567, 118432
62. Ulkoski, D. *et al.* (2019) Recent advances in polymeric materials for the delivery of RNA therapeutics. *Expert Opin. Drug Deliv.* 16, 1149–1167
63. Akinc, A. *et al.* (2005) Exploring polyethylenimine-mediated DNA transfection and the proton sponge hypothesis. *J. Gene Med.* 7, 657–663
64. Kargaard, A. *et al.* (2019) Polymeric siRNA gene delivery – transfection efficiency versus cytotoxicity. *J. Control. Release* 316, 263–291
65. Chen, S. and Jin, T. (2016) Poly-cross-linked PEI through aromatically conjugated imine linkages as a new class of pH-responsive nucleic acids packing cationic polymers. *Front. Pharmacol.* 7, 15
66. Zhao, Z. *et al.* (2019) Development of a biocompatible copolymer nanocomplex to deliver VEGF siRNA for triple negative breast cancer. *Theranostics* 9, 4508–4524
67. Uchida, H. *et al.* (2011) Odd-even effect of repeating aminoethylene units in the side chain of N-substituted polyaspartamides on gene transfection profiles. *J. Am. Chem. Soc.* 133, 15524–15532
68. Suma, T. *et al.* (2012) Enhanced stability and gene silencing ability of siRNA-loaded polyion complexes formulated from polyaspartamide derivatives with a repetitive array of amino groups in the side chain. *Biomaterials* 33, 2770–2779
69. Uchida, S. *et al.* (2013) In vivo messenger RNA introduction into the central nervous system using polyplex nanomicelle. *PLoS One* 8, e56220
70. Uchida, S. *et al.* (2016) Systemic delivery of messenger RNA for the treatment of pancreatic cancer using polyplex nanomicelles with a cholesterol moiety. *Biomaterials* 82, 221–228
71. Molinaro, R. *et al.* (2013) Polyethylenimine and chitosan carriers for the delivery of RNA interference effectors. *Expert Opin. Drug Deliv.* 10, 1653–1668
72. Wang, Q.Z. *et al.* (2006) Protonation constants of chitosan with different molecular weight and degree of deacetylation. *Carbohydr. Polym.* 65, 194–201
73. Vauthier, C. *et al.* (2013) Chitosan-based nanoparticles for in vivo delivery of interfering agents including siRNA. *Curr. Opin. Colloid Interface Sci.* 18, 406–418
74. Song, Y. *et al.* (2018) Combination antitumor immunotherapy with VEGF and PIGF siRNA via systemic delivery of multifunctionalized nanoparticles to tumor-associated macrophages and breast cancer cells. *Biomaterials* 185, 117–132
75. Soliman, O.Y. *et al.* (2020) Efficiency of chitosan/hyaluronan-based mRNA delivery systems in vitro: influence of composition and structure. *J. Pharm. Sci.* 109, 1581–1593
76. Cao, Y. *et al.* (2019) Recent advances in chitosan-based carriers for gene delivery. *Mar. Drugs* 17(6)
77. Du, L. *et al.* (2018) The study of relationships between pKa value and siRNA delivery efficiency based on tri-block copolymers. *Biomaterials* 176, 84–93
78. Tang, H. *et al.* (2018) Recent development of pH-responsive polymers for cancer nanomedicine. *Molecules* 24, 4
79. Xu, X. *et al.* (2016) Ultra-pH-responsive and tumor-penetrating nanoplatform for targeted siRNA delivery with robust anti-cancer efficacy. *Angew. Chem. Int. Ed. Engl.* 55, 7091–7094
80. Ma, X. *et al.* (2014) Ultra-pH-sensitive nanoprobe library with broad pH tunability and fluorescence emissions. *J. Am. Chem. Soc.* 136, 11085–11092
81. Shobaki, N. *et al.* (2018) Mixing lipids to manipulate the ionization status of lipid nanoparticles for specific tissue targeting. *Int. J. Nanomedicine* 13, 8395–8410
82. Pei, D. and Buyanova, M. (2019) Overcoming endosomal entrapment in drug delivery. *Bioconjug. Chem.* 30, 273–283
83. Vermeulen, L.M.P. *et al.* (2018) Endosomal size and membrane leakiness influence proton sponge-based rupture of endosomal vesicles. *ACS Nano* 12, 2332–2345
84. Hinze, C. and Boucrot, E. (2018) Endocytosis in proliferating, quiescent and terminally differentiated cells. *J. Cell Sci.* 131
85. Zhou, K. *et al.* (2011) Tunable, ultrasensitive pH-responsive nanoparticles targeting specific endocytic organelles in living cells. *Angew. Chem. Int. Ed. Engl.* 50, 6109–6114
86. Schonherr, D. *et al.* (2015) Characterisation of selected active agents regarding pKa values, solubility concentrations and pH profiles by SiriusT3. *Eur. J. Pharm. Biopharm.* 92, 155–170
87. Tanaka, H. and Sakamoto, Y. (1993) Polyelectrolyte titration using fluorescent indicator. I. Direct titration of anionic and cationic polyelectrolytes with 10^{-4} N standard solutions. *J. Polym. Sci. A Polym. Chem.* 31, 2687–2691
88. Walsh, C.L. *et al.* (2013) Synthesis, characterization, and evaluation of ionizable lysine-based lipids for siRNA delivery. *Bioconjug. Chem.* 24, 36–43
89. Yamamoto, N. *et al.* (2016) Novel pH-sensitive multifunctional envelope-type nanodevice for siRNA-based treatments for chronic HBV infection. *J. Hepatol.* 64, 547–555
90. Ansell, S.M. and Du, X. Acuitas Therapeutics Inc. Novel lipids and lipid nanoparticle formulation for delivery of nucleic acids, WO2017075531A1